Applied Radiation and Isotopes 206 (2024) 111260

Contents lists available at ScienceDirect

Applied Radiation and Isotopes

journal homepage: www.elsevier.com/locate/apradiso

A series of high-sensitivity radon detection systems and their applications in nitrogen as well as the boil-off liquid nitrogen measurement

Fan Wang [a], Hao Wang [a,b], Zhi Zeng [c], Jinmin Yang [b], Kang Peng [a,b], Lei Zhang [b,*], Qiuju Guo [a]

[a] State Key Laboratory of Nuclear Physics and Technology, School of Physics, Peking University, Beijing, 100871, China
[b] State Key Laboratory of NBC Protection for Civilian, Beijing, 102205, China
[c] Key Laboratory of Particle and Radiation Imaging (Ministry of Education) and Department of Engineering Physics, Tsinghua University, Beijing, 100084, China

ARTICLE INFO

Keywords:
High-sensitivity radon detection
Electrostatic collection
Activated charcoals
Nitrogen
Boil-off liquid nitrogen

ABSTRACT

In modern rare-event search experiments such as neutrino experiments and dark matter search experiments, radon is one of the most important radiation backgrounds since it can emanate from nearly all the materials containing radium and migrate freely in the experiment system. To support the China Dark Matter Experiment (CDEX) at China Jinping Underground Laboratory (CJPL), a series of high-sensitivity radon detection systems with different electrostatic collection chambers were designed, and radon in nitrogen as well as boil-off liquid nitrogen was measured after accurate calibration and enrichment. Results showed that the calibration factors were 2.1 ± 0.2 (counts/h)/(Bq/m^3), 21.1 ± 0.7 (counts/h)/(Bq/m^3), 186.2 ± 2.2 (counts/h)/(Bq/m^3), 387 ± 7 (counts/h)/(Bq/m^3) and the 90% confidence level detection limits were 27.22 mBq/m^3, 1.89 ~ 3.06 mBq/m^3, 0.41 ~ 0.68 mBq/m^3, 0.44 mBq/m^3 for CJPL-HR2, CJPL-HR20, CJPL-HR140 and CJPL-HR300 measurement systems, respectively. Combined with an enrichment system consisting of twenty g CarboACT activated charcoals in a cold trap, the lower level detection limit (LLD) of typical No.1 CJPL-HR140 could reach 1.8 μBq/m^3 with three days' enrichment time and three days' measurement time at 20 L/min sampling flowrate. For verification and application, the radon activity concentrations in nitrogen were 0.6 ~ 1.9 mBq/m^3 with an average of 1.1 ± 0.1 mBq/m^3.While in boil-off liquid nitrogen, the radon activity concentrations ranged from 0.04 to 0.62 mBq/m^3, and they were significantly lower in old-decayed liquid nitrogen compared to newly-filled liquid nitrogen, with a nearly five-fold decrease.

1. Introduction

The China Dark Matter Experiment (CDEX) aims at direct searches of light Weakly Interacting Massive Particles (WIMPs) at the China Jinping Underground Laboratory (CJPL) with an overburden of about 2400 m of rock (Ma et al., 2020). The experimental setup will adopt germanium detector arrays deploying in a liquid nitrogen tank with 13 m in diameter and 13 m in height, which acts as a cooling medium for germanium arrays and as passive shielding material against ambient radioactivity simultaneously (Ma et al., 2020). Radon emanating from the stainless steel tank and detector materials could migrate in the liquid nitrogen and decay to a series of radon progeny with different half-lives, which is one of the most important radiation backgrounds for CDEX. Therefore, radon must be carefully suppressed and accurately evaluated at an extremely low level (μBq/m^3) in the liquid nitrogen tank in the CDEX experiment.

For the demand of ultra-low-background and high-sensitivity radon detection, different laboratories have developed different measurement systems with different methods based on their own needs, mainly including the large-volume scintillation chamber (Wójcik and Wlazło, 1994), the electrostatic radon detectors (Takeuchi et al., 1999; Kiko, 2001; Nakano et al., 2017; Pelczar et al., 2021; Chen et al., 2022), the ultra-low background proportional counters (Wink et al., 1993) and the cryogenic radon detectors (Wójcik and Zuzel, 2008), which reviewed mainly by M. Wojcik et al. (2017) and some new systems developed recently. Among these measurement techniques, electrostatic radon detectors are most widely adopted in practice due to their distinguishing radon from thoron and suitability for continuous measurement as well as discrete measurement. Such as the electrostatic radon detectors established in the Super-Kamiokande experiment in 1999, which possessed a 70 L electrostatic collection chamber with −2000 V high volume and an 18×18 mm Si-PIN detector for radon measurement, and the 90%

* Corresponding author.
E-mail address: swofely@pku.edu.cn (L. Zhang).

https://doi.org/10.1016/j.apradiso.2024.111260
Received 17 October 2023; Received in revised form 17 February 2024; Accepted 26 February 2024
Available online 28 February 2024

confidence level detection limit could be as low as 1.4 mBq/m^3 (Takeuchi et al., 1999). In 2002, another electrostatic radon detector with a 418 L collection chamber was constructed in the Borexino experiment, and the detection limit could be lower than 1 mBq/m^3 (Kiko, 2001). After that, a new 80 L electrostatic radon detector was built for improvement in 2017 for the Super-Kamiokande experiment, and a lower background and a lower detection limit were achieved (Nakano et al., 2017). Recently, a 450 L electrostatic radon detector with −8000 V high volume has been developed in the Darkside experiment, and its detection limit could be as low as 0.05 mBq/m^3 (Pelczar et al., 2021). In 2022, an electrostatic radon detector with a 41.5 L electrostatic collection chamber and −700 V high volume was established in the JUNO experiment, where the detection limit could reach 0.71 mBq/m^3 respectively (Chen et al., 2022).

To support the CDEX experiment and meet various needs of radon detection in nitrogen, liquid nitrogen, other materials, and clean rooms in CJPL, a series of high-sensitivity radon detection systems were designed and tested in this paper. Considering the need for μBq/m^3-level radon concentration measurement, a "cold trap" enrichment system was also integrated with those electrostatic radon detectors, and the application for low-level radon activity concentration evaluation in nitrogen and liquid nitrogen was also shown in this paper.

2. Materials and methods

2.1. Electrostatic radon monitors

Four types of electrostatic radon monitors have been established, which were CJPL-HR2, CJPL-HR20, CJPL-HR140, and CJPL-HR300, respectively. All of them were constituted of a Si-PIN photodiode (S3204-09&S3584-09, Hamamatsu Co, Japan (Hamamatsu Photonics Co)), a charge-sensitive preamplifier (AMP), a multi-channel analyzer (MCA), and a multi-control unit (MCU) and an electrostatic collection chamber, just as shown in Fig. 1. A high voltage module supplied negative voltage on Si-PIN surface, and then the positive radon progenies $^{218}Po^+$, $^{214}Pb^+$, $^{214}Bi^+$ could be collected on the surface of the detector. Those α particles emitted from ^{218}Po, ^{214}Po, and thoron progeny could be recorded by the detector, and the alpha spectrum was analyzed and recorded by MCA and MCU automatically. The specific parameters of those four types and seven high-sensitivity electrostatic radon monitors are shown in Table 1. The inner effective volume was measured by the PVT method accurately, which is based on the air isothermal expansion after changing of inner effective volume and lead to the change of pressure and temperature simultaneously (Yi-fan et al., 2020), and the high voltage was recorded simultaneously. The whole system was designed as stainless steel vacuum chambers, and the leakage rate could be as low as 10^{-9} Pa m^3/s.

Because the region of interest (ROIs) of ^{214}Po is mostly "clean" without being influenced by thoron progeny, only 7.69 MeV α particles

Table 1
Specific parameters of seven high-sensitivity electrostatic radon monitors with four different types.

Model	Size of Si-PIN photodiode	Volume of electrostatic collection chamber (L)	Voltage (V)
CJPL-HR2 (No.1)	18 × 18 mm	2.6 ± 0.1	−1800
CJPL-HR2 (No.2)	18 × 18 mm	2.6 ± 0.1	−1800
CJPL-HR20 (No.1)	18 × 18 mm	23.7 ± 0.2	−2000
CJPL-HR20 (No.2)	18 × 18 mm	23.9 ± 0.1	−2000
CJPL-HR140 (No.1)	28 × 28 mm	139.7 ± 0.8	−3000
CJPL-HR140 (No.2)	28 × 28 mm	139.5 ± 0.7	−3000
CJPL-HR300	28 × 28 mm	329.2 ± 1.9	−5000

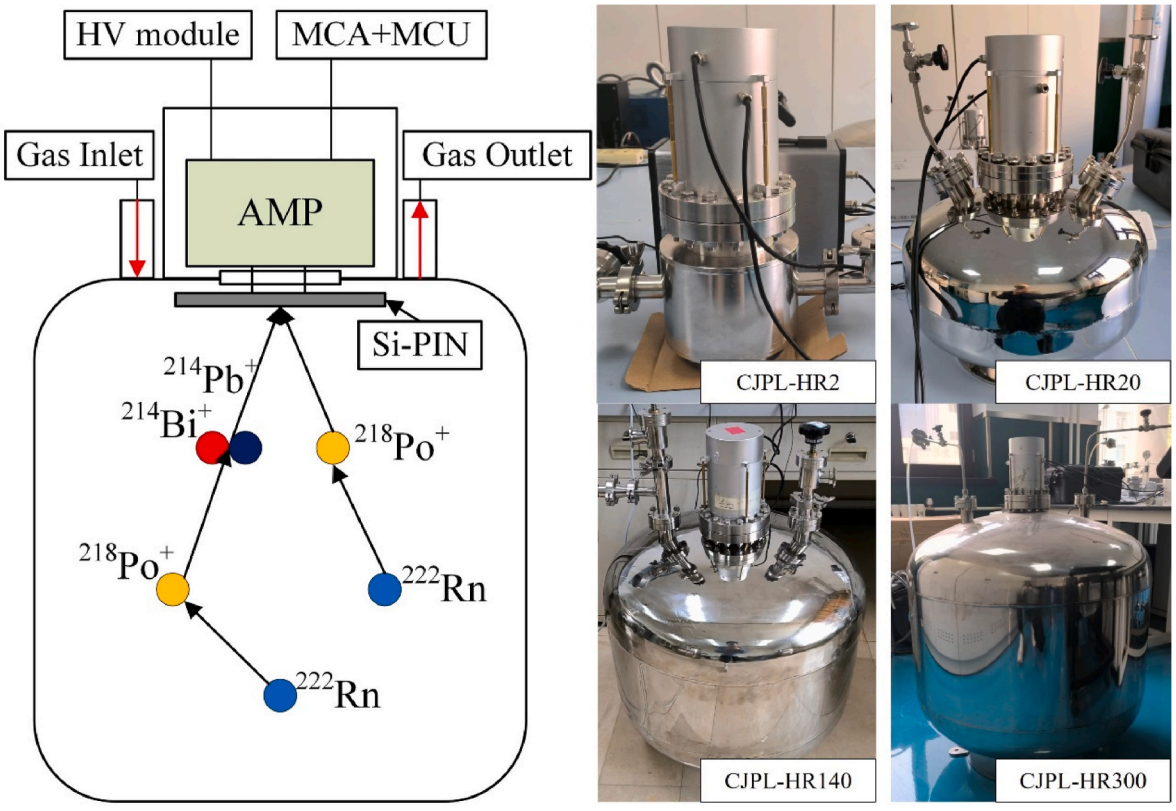

Fig. 1. Schematic diagram and pictures of those high-sensitivity electrostatic radon detectors.

are used for radon activity concentration calculation (Nakano et al., 2017). For continuous working mode, ignoring the concentration variety during sampling and measurement progress and ignoring the uncertainty of measurement time T, the radon activity concentration can be calculated by the following equation, and its uncertainty could be calculated through error transfer formula considering the average background B, the uncertainty of calibration factor σ_{C_F} and the uncertainty of total counting N(T).

$$C_{Rn} = \frac{N(T) - BT/24}{TC_F} \tag{1}$$

$$\sigma_{C_{Rn}} = \sqrt{\frac{\sigma_{C_F}^2}{C_F^2} C_{Rn}^2 + \frac{N(T) + BT/24}{T^2 C_F^2}} \tag{2}$$

Where C_{Rn} is the radon activity concentration (Bq/m^3) and $\sigma_{C_{Rn}}$ is its uncertainty. N(T) is the total counts in the ROIs during measurement cycle T (h) and B is the background counting rate (counts/d). C_F is the calibration factor [(counts/h)/(Bq/m^3)], which is the net counts of ^{214}Po per unit radon activity concentration, and σ_{C_F} is its uncertainty, which is gotten through repeated calibration and ignore the uncertainty of the reference monitor.

For discrete working mode, in which radon is injected into the chamber once and measured for T, the radon activity concentration and its uncertainty could be calculated by the following equation:

$$C_{Rn} = \frac{\lambda}{C_F} \bullet \frac{N(T) - BT/24}{1 - e^{-\lambda T}} \tag{3}$$

$$\sigma_{C_{Rn}} = \sqrt{\frac{\sigma_{C_F}^2}{C_F^2} C_{Rn}^2 + \frac{\lambda^2}{C_F^2} \bullet \frac{N(T) + BT/24}{(1 - e^{-\lambda T})^2}} \tag{4}$$

Where λ is the decay constant of radon ($\lambda \approx 7.56 \times 10^{-3}$ h^{-1}).

The lower level detection limit (LLD) of radon concentration (Bq/m^3) of the radon detector for 72 h measurement with a confidence level of 95% is calculated by the following equation as defined by Currie (1968) (Currie, 1968) and ISO11929 (International Organization for Standardization, 2019):

$$LLD \approx \frac{2.71 + 4.65\sqrt{M_B}}{TC_F} \tag{5}$$

Where M_B is the background counts of ROIs. For continuous working mode, it's measured in a gas-flow environment using "cold-trapped" boil-off liquid nitrogen. For discrete working mode, it's measured integrally with no radon environment, which is realized by filling with extremely low-level boil-off liquid nitrogen and last for 72 h.

For comparison with other measurement systems, the 90% confidence level (CL) detection limit (Bq/m^3) of the radon detector is also given using the following equation (Mitsuda et al., 2003):

$$L_c = \frac{1.64\sigma_B}{C_F} \tag{6}$$

Where L_C and σ_B are the 90% CL detection limit and the uncertainty of the background (counts/d), which means the radon higher than L_C·V (Bq) could usually be distinguished from the background.

2.2. μBq/m^3-level radon measurement system

Due to the detection limit of single-chamber electrostatic radon monitors, an enrichment system of activated charcoals in a "cold trap" should be used together with those electrostatic radon monitors for μBq/m^3-level radon detection. Due to its low intrinsic background and high adsorption at liquid nitrogen temperature (Wang et al., 2023), the CarboACT activated charcoal (Carbo-act International, the Netherlands (Carboact charcoal specification)) was adopted in the μBq/m^3-level radon detection system, which was designed and established in this paper, just as shown in Fig. 2. In this system, ten g CarboACT and twenty g CarboACT were separately filled in different stainless steel tubes for filtration and enrichment respectively. In the absorption process, as shown by the upper part of Fig. 2, twenty g CarboACT was immersed in the liquid nitrogen and continuously adsorbed radon in gas samples at a stable flowrate of nearly 20 L/min, which was also recorded by a flowmeter. In the desorption process, the twenty g CarboACT was heated to 200 °C, and then the desorbed radon was transferred to the radon monitor by boil-off liquid nitrogen gas. To obtain extremely low-level nitrogen gas, the boil-off nitrogen from a 240 L liquid nitrogen tank passed through a ten g CarboACT with a flowrate of nearly 10 L/min, and then the radon background could be ignored. Because radon dynamic adsorption coefficient k_α of CarboACT was nearly 1.2×10^{13} L/g at liquid nitrogen temperature (77 K) (Wang et al., 2023), and the breakthrough time ($\tau = mk_\alpha/\upsilon$) at 77 K was nearly 1.2×10^{13} min, which was too much longer than radon's half-life (3.82 days). Thus, nearly all radon was adsorbed in activated charcoals during adsorption process. During desorption process, the CarboACT activated charcoals were heated to 200 °C with the dynamic adsorption coefficient k_α 0.4 ± 0.1 L/g (Wang et al., 2023), then more than 99.9% (estimated simply by $1 - \left(\frac{1}{2}\right)^{\frac{V}{mk_\alpha}} = 1 - \left(\frac{1}{2}\right)^{\frac{140L}{20g \times 0.4L/g}} > 99.9\%$) of radon was transported to radon chamber with 140 L boil-off nitrogen.

Considering the enrichment and decay during the enrichment and detection process, the radon activity concentration and uncertainty in gas samples should be calculated as follows:

$$C_{Rn}(sam) = \frac{\lambda V_{cha}}{\upsilon(1 - e^{-\lambda t})} \bullet C_{Rn} = \frac{\lambda^2 V_{cha}}{\upsilon C_F} \bullet \frac{N(T) - BT/24}{(1 - e^{-\lambda t}) \bullet (1 - e^{-\lambda T})} \tag{7}$$

$$\sigma_{C_{Rn}}(sam) = \sqrt{\left(\frac{\sigma_{C_{Rn}}}{C_{Rn}}\right)^2 + \left(\frac{\sigma_{V_{cha}}}{V_{cha}}\right)^2 + \left(\frac{\sigma_{V_{sam}}}{V_{sam}}\right)^2} C_{Rn}(sam) \tag{8}$$

Where C_{Rn}(sam) is the radon activity concentration of sample gas (Bq/m^3) and $\sigma_{C_{Rn}}$(sam) is the uncertainty of C_{Rn}(sam), which is mainly contributed by the uncertainty of C_{Rn}, V_{cha} and V_{sam}. V_{cha} is the inner volume (L) of the electrostatic collection chamber and $\sigma_{V_{cha}}$ is its uncertainty. V_{sam} is the sampling volume (L) in adsorption process and $\sigma_{V_{sam}}$ is its uncertainty. υ is the sampling flowrate (L/min), t is the adsorption time (h), and T is the integrated measurement time (h).

Define an enrichment factor K as the ratio of the radon concentration in the measurement chamber after accumulation and transfer to the radon concentration in gas samples, then the radon activity concentration of gas samples could be calculated as follows:

$$C_{Rn}(sam) = \frac{C_{Rn}}{K} \tag{9}$$

$$K = \frac{\upsilon}{\lambda \bullet V_{cha}} \bullet \left(1 - e^{-\lambda t}\right) \tag{10}$$

Actually, the enrichment factor K reflects the proportion brought by the enrichment and transfer process, and K is increased with the enrichment time t at a fixed flowrate υ of 20 L/min. However, there is an upper limit of t due to the decay during the enrichment progress. When t is as long as nearly infinite, $K = \upsilon/(\lambda \bullet V_{cha})$. When t is relatively small, decay correction could be ignored, and $K = \upsilon t/V_{cha}$ for simplification.

2.3. Calibration and application in nitrogen as well as boil-off liquid nitrogen

Due to nitrogen and liquid nitrogen being widely used in CJPL, high-sensitivity radon measurement systems were applied to measure the radon activity concentration in nitrogen as well as boil-off liquid nitrogen. First, the calibrations of the electrostatic radon monitors were performed in a high pure nitrogen environment, and an AlphaGUARD PQ2000 (Saphymo, France) with a Verification Coefficients of 0.997

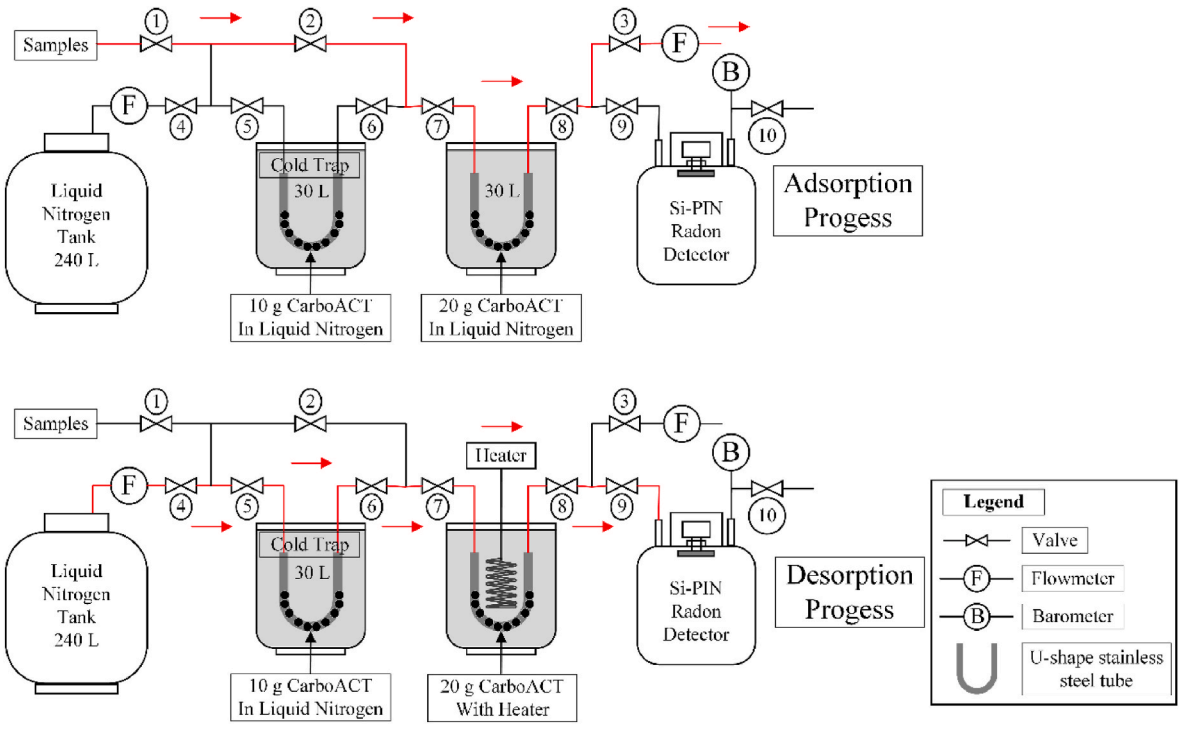

Fig. 2. Schematic diagram of the μBq/m^3-level radon measurement system.

(Saphymo) was used as a transfer reference standard, just as shown in Fig. 3. The radon activity concentration could be traced back to the National Radon Standard of Metrological Institute of China. During the calibration, the flowrate was set to nearly 2 L/min and kept stable. Then, the radon activity concentration from the flow-through ^{222}Rn source (a solid ^{226}Ra source with an activity of nearly 3000 Bq) was 200 ± 19 Bq/m^3. The calibration factors and their uncertainties were gotten through calculation, where the means and standard deviations of the ratios of the measured net counts in the ROIs of ^{214}Po to the measured radon activity concentrations from the AlphaGUARD were considered.

For evaluation of the intrinsic background of the electrostatic radon monitors, the boil-off liquid nitrogen passed through a "cold trap" was used as the "free-of-radon" gas and filled in the electrostatic collection chambers. Then, the chambers were sealed and measured continuously for more than a week. Only the initial 3-day counts were taken for background calculation and usually 3 to 5 times repeated measurements were carried out for different radon monitors. Because radon in the boil-off liquid nitrogen was removed by activated charcoals in a "cold trap", the background results could be regarded as only those exhaled from inner chamber materials and detectors.

In this paper, the radon activity concentrations of industrial nitrogen (3N, 99.2%–99.999%), high-purity nitrogen (4N, 99.9%–99.999%), and the boil-off liquid nitrogen were measured. The nitrogen and liquid nitrogen were supplied by JINGHUI GAS Co., China (JINGHUI GAS and China). The boil-off liquid nitrogen was generated by the 240 L liquid tank (YDZ-240, Sichuan Shanli Cryogenic Equipment Co, China (YDZ-240)), which could be newly filled and left to stand for a month. Each nitrogen sample would be measured repeatedly to confirm the results.

3. Results and discussion

3.1. C_F, LLD, and L_C of the electrostatic radon monitors

Through calibration and background measurements, the calibration factor, average background (C_F), lower level detection limit (LLD), and 90% confidence level detection limit (L_C) were obtained, and those parameters are given in Table 2. For matching the typical 72-h measurement cycle, the background counting rates were taken as the ratio of the initial 3-day counts to 3 days and the average backgrounds were the average of the background counting rates obtained in 3–5 times repeated measurements, which is shown in Table 2. For CJPL-HR2, CJPL-HR20, CJPL-HR140, CJPL-HR300, the average calibration factors were 2.1 ± 0.2 (counts/h)/(Bq/m^3), 21.1 ± 0.7 (counts/h)/(Bq/

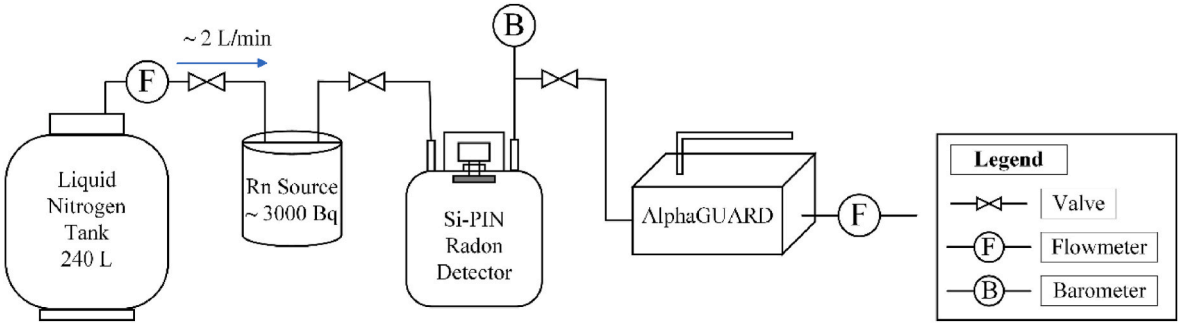

Fig. 3. Schematic diagram of the calibration progress for electrostatic radon monitors.

Table 2
Parameters of different electrostatic radon monitors.

Model	Average background (counts/d)	calibration factor [(counts/h)/(Bq/m^3)]	LLD (72h) (mBq/m^3)	L_C (mBq/m^3)
CJPL-HR2 (No.1)	0.7	2.1 ± 0.2	62.49	27.22
CJPL-HR2 (No.2)	0.7	2.1 ± 0.2	62.49	27.22
CJPL-HR20 (No.1)	0.3	19.8 ± 0.9	5.00	1.89
CJPL-HR20 (No.2)	1.0	22.3 ± 1.0	6.70	3.06
CJPL-HR140 (No.1)	1.3	188.8 ± 4.2	0.87	0.41
CJPL-HR140 (No.2)	3.3	183.6 ± 1.6	1.31	0.68
CJPL-HR300	6.3	387 ± 7	0.82	0.44

m^3), 186.2 ± 2.2 (counts/h)/(Bq/m^3), 387 ± 7 (counts/h)/(Bq/m^3) and the LLDs in 72-h measurement cycle were 62.49 mBq/m^3, 5.00 ~ 6.70 mBq/m^3, 0.87 ~ 1.31 mBq/m^3, 0.82 mBq/m^3, respectively. Results also showed that the calibration factors and average backgrounds of the electrostatic radon monitors increased with the increase of chamber volume, while the LLDs and L_C decreased with the increase of chamber volume.

For the electrostatic radon monitors of the same chamber size, the average backgrounds were relatively close, and the difference may be attributed to the slight difference in chamber cleanness and airtightness. Similarly, for the electrostatic radon monitors of the same type, the calibration factors were also close, and the little difference may come from the slight difference of the electrostatic fields, which was mainly caused by the Si-PIN photodiodes position which were manually installed.

For comparison, similar parameters of the electrostatic radon monitors in other experiments were summarized in Table 3. Compared with those electrostatic radon monitors, the background of our monitors was nearly the same level with different measurement time, and the sensitivity could be comparable with different inner volumes of chambers. The L_C of CJPL-HR140 and CJPL-HR300 all reached the sub-mBq/m^3 levels, just like those in the Super-Kamiokande and JUNO experiments.

Table 3
Parameters of similar electrostatic radon monitors in other experiments.

electrostatic radon monitors	Volume (L)	Voltage (V)	Average background (counts/d)	calibration factor [(counts/h)/(Bq/m^3)]	L_C (mBq/m^3)
Super-K (Takeuchi et al., 1999)	70	−2000	2.4 (2 months)	91.7	1.4
Borexino (Kiko, 2001)	418	−30000	<2	1125	<1
Super-K (Nakano et al., 2017)	80	−2000	0.74 (156 days)	93.8	0.54
DarkSide (Pelczar et al., 2021)	450	−8000	3.0 (24.8 days)	579.2	0.05
Super-K (Okamoto et al., 2021)	80	−2000	0.57 (28 days)	103.3	\
JUNO (Chen et al., 2022)	41.5	−700	0.7 (30 days)	67.0	0.71

3.2. LLDs of the μBq/m^3-level radon measurement systems

In order to evaluate the theoretical measurement capabilities of the μBq/m^3-level radon measurement systems, take CJPL-HR140 (No.1) as an example to calculate the enrichment factor Ks and LLDs. Calculation results are shown in Table 4 and Fig. 4. The flowrate was set and controlled to 20 L/min stably. According to the results, the enrichment factor K increased when the enrichment time became longer, and for the LLDs, they decreased as the enrichment time and measurement time increased. If the enrichment time was 3 days, enrichment factor K could reach 477, and the LLDs could be lowered by nearly 500 times. Theoretically, when the enrichment time was 3 days and the measurement time was 3 days, the LLD of CJPL-HR140 (No.1) could reach 1.8 μBq/m^3, which was in accordance with our design and could meet the needs of the CJPL experiment. Under the same conditions, the average LLDs were 0.13 mBq/m^3, 12.3 μBq/m^3, and 1.7 μBq/m^3 for CJPL-HR2, CJPL-HR20, and CJPL-HR300.

Although CJPL-HR140 (No.1) has been calculated as an example in Table 4, each type of electrostatic radon monitor could be combined with the radon enrichment system. When the radon monitor with a smaller collection chamber is chosen, the enrichment factor K will be larger at the same enrichment time and flowrate. However, too small a chamber is not conducive to transferring all radon. Thus, the volume of the electrostatic collection chamber should match the mass of activated charcoal.

3.3. Measurement results of nitrogen and boil-off liquid nitrogen gas

For application and to test the μBq/m^3-level radon measurement systems, three kinds of nitrogen samples: industrial purity nitrogen, high-purity nitrogen, and boil-off liquid nitrogen, were measured in this study. In practice, both CJPL-HR140 (No.1) and CJPL-HR140 (No.2) were used. The volume of a cylinder of nitrogen samples was nearly 6 m^3, and each cylinder could be measured twice. Thus, the enrichment volumes of nitrogen samples were about 2 ~ 3 m^3. As for the boil-off liquid nitrogen, the enrichment volumes could be much larger to meet the measurement needs. The measurement results and uncertainties of nitrogen and the boil-off liquid nitrogen are obtained according to equations (7) and (8), which are shown in Table 5 and Table 6, respectively. The results in Table 6 are also presented in Fig. 5.

According to the measurement results in Tables 5 and 6, the radon concentrations of the boil-off liquid nitrogen were obviously lower than those of nitrogen samples in nitrogen cylinders, which were 0.04 ~ 0.62 mBq/m^3 and 0.6 ~ 1.9 mBq/m^3 respectively. The radon activity concentration of newly-filled liquid nitrogen was nearly 3 times lower than

Table 4
The Enrichment factor K and the LLDs of CJPL-HR140 (No.1) monitor at different enrichment time (flowrate = 20 L/min).

Enrichment time	Enrichment factor K	Measurement time		
		1 day	2 days	3 days
		LLD (mBq/m^3)		
0 h	1.0	1.77	1.13	0.87
1 h	8.6	0.21	0.13	0.10
		LLD (μBq/m^3)		
12 h	99	17.9	11.4	8.9
1 day	189	9.4	6.0	4.6
3 days	477	3.7	2.4	1.8
5 days	678	2.6	1.7	1.3
7 days	818	2.2	1.4	1.1

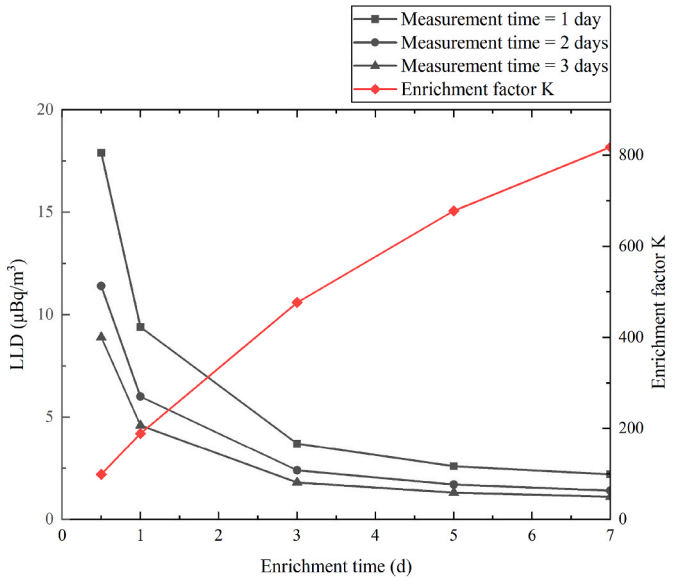

Fig. 4. The Enrichment factor K and the LLDs of CJPL-HR140 (No.1) monitor at different enrichment time (flowrate = 20 L/min).

Table 5
Measurement results of the radon activity concentration of nitrogen gas.

Type of nitrogen sample	Nitrogen sample	Sampling volume (m^3)	Radon concentration (mBq/m^3)	Average radon concentration (mBq/m^3)
Industrial purity nitrogen (3N)	Nitrogen cylinder 1	2.65 ± 0.13	0.9 ± 0.2	1.0 ± 0.1
		2.00 ± 0.10	1.1 ± 0.2	
	Nitrogen cylinder 2	2.47 ± 0.12	0.9 ± 0.2	
High-purity nitrogen (4N)	Nitrogen cylinder 3	2.55 ± 0.13	1.9 ± 0.2	1.2 ± 0.1
		2.30 ± 0.12	1.5 ± 0.2	
	Nitrogen cylinder 4	2.63 ± 0.13	0.7 ± 0.1	
		2.74 ± 0.14	0.6 ± 0.1	

Table 6
Measurement results of the radon activity concentration of the boil-off liquid nitrogen.

Boil-off liquid nitrogen	Sampling volume (m^3)	Radon concentration (mBq/m^3)	Average radon concentration (mBq/m^3)
Newly-filled	17.99 ± 0.90	0.22 ± 0.03	0.37 ± 0.03
	8.73 ± 0.44	0.62 ± 0.07	
	6.09 ± 0.30	0.28 ± 0.07	
Old-decayed	7.03 ± 0.35	0.04 ± 0.02	0.06 ± 0.02
	5.72 ± 0.29	0.07 ± 0.03	

that of nitrogen gas. For nitrogen samples in nitrogen cylinders, the average radon concentrations of industrial nitrogen and high-purity nitrogen were 1.0 ± 0.1 mBq/m^3 and 1.2 ± 0.1 mBq/m^3, which showed no significant difference between the two kinds of nitrogen samples. However, the radon concentrations may be quite different between different nitrogen cylinders, such as nitrogen cylinders 3 and 4. The difference may be attributed to the cleanness and materials of nitrogen cylinders and the filling process.

As for the boil-off liquid nitrogen, the gas samples under two conditions were measured, which were new-filled and old-decayed, just as

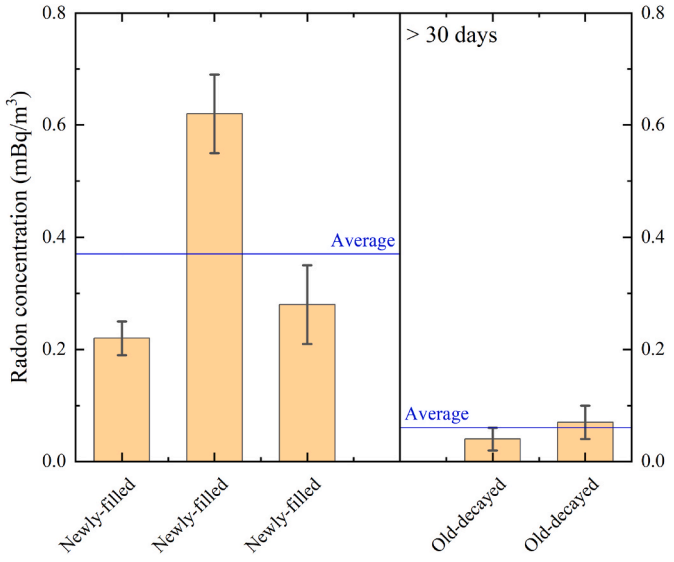

Fig. 5. Measurement results of the radon activity concentration of the boil-off liquid nitrogen.

shown in Table 6 and Fig. 5. For new-filled liquid nitrogen, the average radon concentration of the boil-off nitrogen was 0.37 ± 0.03 mBq/m^3. After the same liquid nitrogen had been left still for a month to decay, the average radon activity concentration of the boil-off gas was 0.06 ± 0.02 mBq/m^3, which was nearly 5 times lower. This finding is quite interesting, and the probable reason might be that when the liquid nitrogen was filled into the liquid nitrogen tank, a small amount of air might enter the tank with liquid nitrogen or through leakage. When the liquid nitrogen was left still for a month, most radon carried into the liquid nitrogen tank decayed, and the radon concentration decreased obviously. The measurement results presented that if we need nitrogen with extremely low radon concentrations, we should choose the boil-off liquid nitrogen, which has been left still for a long time in the liquid nitrogen tank. Of course, the liquid nitrogen tank must be "clean" first. Moreover, it could be even lower by filtering through activated charcoals at low temperatures ("cold trap"), and then a "free-of-radon" nitrogen gas might be obtained.

4. Conclusion

For serving the CDEX experiment related to the radon issue, a series of high-sensitivity radon measurement systems with different electrostatic radon monitors have been established and calibrated in our laboratory. For CJPL-HR2, CJPL-HR20, CJPL-HR140, CJPL-HR300, the average calibration factors were 2.1 ± 0.2 (counts/h)/(Bq/m^3), 21.1 ± 0.7 (counts/h)/(Bq/m^3), 186.2 ± 2.2 (counts/h)/(Bq/m^3), 387 ± 7 (counts/h)/(Bq/m^3) and the LLDs in 72-h measurement cycle were 62.49 mBq/m^3, 5.00 ~ 6.70 mBq/m^3, 0.87 ~ 1.31 mBq/m^3, 0.82 mBq/m^3, respectively. Combined with an enrichment system consisting of twenty g CarboACT activated charcoals in the cold trap, the LLD of the No.1 CJPL-HR140 could reach 1.8 $\mu Bq/m^3$ with three days' enrichment time and three days' measurement time at a 20 L/min sampling flowrate.

For application, the radon activity concentrations of industrial nitrogen, high-purity nitrogen, and boil-off liquid nitrogen have been measured in this study. For industrial nitrogen and high-purity nitrogen, the average radon concentrations were 1.0 ± 0.1 mBq/m^3 and 1.2 ± 0.1 mBq/m^3, and no significant difference was found. The average radon activity concentration was 0.37 ± 0.03 mBq/m^3 for newly-filled liquid nitrogen and could be lowered to 0.06 ± 0.02 mBq/m^3 after a month's decay, which could be further lower by filtering through activated charcoals at low temperatures. Those measurement systems can be used

for various radon detection in CJPL, such as clean room air monitor, radon removal efficiency evaluation, radon emanation rate measurement, and so on. More actual measurement results will be given in the future.

CRediT authorship contribution statement

Fan Wang: Writing – review & editing, Writing – original draft, Validation, Formal analysis, Data curation. **Hao Wang:** Validation, Formal analysis, Data curation. **Zhi Zeng:** Resources, Funding acquisition. **Jinmin Yang:** Validation, Formal analysis, Data curation. **Kang Peng:** Data curation. **Lei Zhang:** Writing – review & editing, Methodology, Investigation, Funding acquisition, Formal analysis, Conceptualization. **Qiuju Guo:** Writing – review & editing, Project administration, Funding acquisition, Formal analysis, Conceptualization.

Declaration of competing interest

The authors have no conflict of interest with any individual, organization, or research institution.

Data availability

Data will be made available on request.

Acknowledgment

We would like to thank the financial support of the CDEX collaboration and the National Natural Science Foundation of China (No. 12275008).

References

Carboact Charcoal Specific., https://www.carboactinternational.com/, Last time accessed: 2023-October-17.

Chen, Y.Y., et al., 2022. A study on the radon removal performance of low background activated carbon. J. Inst. Met. 17, P02003 https://doi.org/10.1088/1748-0221/17/02/P02003.

Currie, L.A., 1968. Limits for qualitative detection and quantitative determination. Application to radiochemistry. Anal. Chem. 40 (3), 586–593.

Hamamatsu Photonics Co, https://www.hamamatsu.com/, Last time accessed: 2023-October-17.

International Organization for Standardization, 2019. Determination of the Characteristic Limits (Decision Threshold, Detection Limit and Limits of the Confidence Interval) for Measurements of Ionizing Radiation-Fundamentals and Application. ISO 11929.

JINGHUI GAS, China, https://www.hyjhqt.com/, Last time accessed: 2023-October-17..

Kiko, J., 2001. Detector for ^{222}Rn measurements in air at the 1 mBq/m3 level. Nucl. Instrum. Methods Phys. Res. 460, 272–277.

Ma, Hao, et al., 2020. CJPL Dark matter experiment: status and prospects. J. Phys. Conf. Ser. 1342, 012067 https://doi.org/10.1088/1742-6596/1342/1/01206.

Mitsuda, C., et al., 2003. Development of super-high sensitivity radon detector for the Super-Kamiokande detector. Nucl. Instrum. Methods A 497, 414.

Nakano, Y., et al., 2017. Measurement of radon concentration in super-kamiokande's buffer gas. Nucl. Instrum. Methods 867, 108–114.

Okamoto, K., et al., 2021. Improvement of Radon Detector Performance by Using a Large-Sized PIN-Photodiode arXiv:2112.06614 [physics.ins-det].

Pelczar, K., et al., 2021. An online radon monitor for low-background detector assembly facilities. Eur. Phys. J. C 81, 86.

Saphymo, Bertin Instrum., https://www.saphymo.com, Last time accessed: 2023-October-17..

Takeuchi, Y., et al., 1999. Development of high sensitivity radon detectors. Nucl. Instrum. Methods 421, 334–341.

Wang, Fan, et al., 2023. Radon dynamic adsorption coefficients of two activated charcoals at different temperatures in nitrogen environment. Appl. Radiat. Isot. 191, 110564.

Wink, R., et al., 1993. The miniaturized proportional counter HD-2(Fe)/(Si) for the GALLEX solar neutrino experiment. Nucl. Instrum. Methods A 329, 541.

Wójcik, M., Wlazło, W., 1994. A high sensitivity scintillation chamber for radon in gas. Nucl. Instrum. Methods 345 (2), 351–355.

Wójcik, M., Zuzel, G., 2008. A high sensitivity large volume cryogenic detector for 222Rn in gas. J. Radioanal. Nucl. Chem. 277, 199–205.

Wojcik, M., et al., 2017. Review of high-sensitivity Radon studies. Int. J. Mod. Phys. A 32, 1743004. https://doi.org/10.1142/S0217751X17430047.

YDZ-240, Sichuan Shanli Cryogen. Equip.Co, China, http://xn–oqq156e.xn–fiqs8s/, Last time accessed: 2023-October-17.

Yi-fan, Y.A.N., et al., 2020. Research on the method of traceability the value of standard radon monitor. Acta Metrol. Sin. 41, No2.